Cell Reports

Report

Complete Loss of Netrin-1 Results in Embryonic Lethality and Severe Axon Guidance Defects without Increased Neural Cell Death

Graphical Abstract

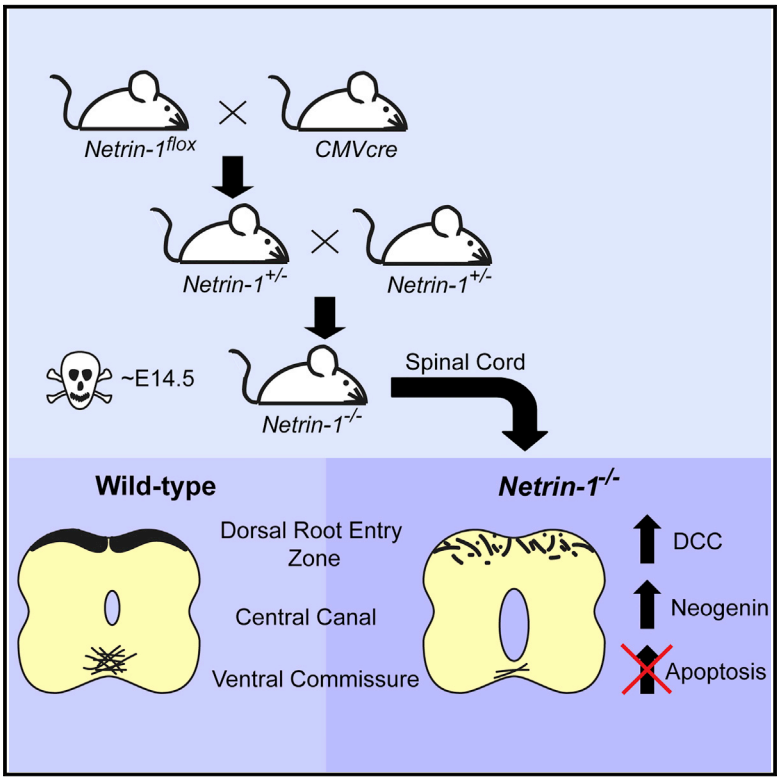

Authors

Jenea M. Bin, Dong Han, Karen Lai Wing Sun, ..., Jean-Francois Cloutier, Artur Kania, Timothy E. Kennedy

Correspondence

timothy.kennedy@mcgill.ca

In Brief

Bin et al. have generated a netrin-1 null mouse that displays phenotypes more severe than those of the reported netrin-1 gene-trap mouse, including embryonic lethality and exacerbated axon guidance defects. No increased apoptosis was detected, indicating that netrin-1 is not an essential dependence ligand, despite increased DCC and neogenin in netrin-1 nulls.

Highlights

- Generated netrin-1 floxed allele and complete netrin-1 null mouse lines
- Complete netrin-1 loss-of-function causes embryonic lethality
- Absence of netrin-1 increases DCC and neogenin protein expression
- Netrin-1 is not an essential dependence ligand in the developing spinal cord

Bin et al., 2015, Cell Reports *12*, 1099–1106
August 18, 2015
http://dx.doi.org/10.1016/j.celrep.2015.07.028

CellPress

Cell Reports
Report

Complete Loss of Netrin-1 Results in Embryonic Lethality and Severe Axon Guidance Defects without Increased Neural Cell Death

Jenea M. Bin,[1,3,6] Dong Han,[1,6] Karen Lai Wing Sun,[1,3] Louis-Philippe Croteau,[2,3,4,5] Emilie Dumontier,[1] Jean-Francois Cloutier,[1,3] Artur Kania,[2,3,4,5] and Timothy E. Kennedy[1,3,*]
[1]Department of Neurology and Neurosurgery, Montreal Neurological Institute, McGill University, Montréal, QC H3A 2B4, Canada
[2]Institut de Recherches Cliniques de Montréal (IRCM), Montréal, QC H2W 1R7, Canada
[3]Integrated Program in Neuroscience, McGill University, Montréal, QC H3A 2B2, Canada
[4]Division of Experimental Medicine, Departments of Anatomy and Cell Biology, and Biology, McGill University Montréal, QC H3A 2B2, Canada
[5]Faculté de Médecine, Université de Montréal, Montréal, QC H3C 3J7, Canada
[6]Co-first author
*Correspondence: timothy.kennedy@mcgill.ca
http://dx.doi.org/10.1016/j.celrep.2015.07.028

SUMMARY

Netrin-1 regulates cell migration and adhesion during the development of the nervous system, vasculature, lung, pancreas, muscle, and mammary gland. It is also proposed to function as a dependence ligand that inhibits apoptosis; however, studies disagree regarding whether netrin-1 loss-of-function mice exhibit increased cell death. Furthermore, previously studied netrin-1 loss-of-function gene-trap mice express a netrin-1-β-galactosidase protein chimera with potential for toxic gain-of-function effects, as well as a small amount of wild-type netrin-1 protein. To unambiguously assess loss of function, we generated netrin-1 floxed and netrin-1 null mouse lines. *Netrin-1*$^{-/-}$ mice die earlier and exhibit more severe axon guidance defects than netrin-1 gene-trap mice, revealing that complete loss of function is more severe than previously reported. *Netrin-1*$^{-/-}$ embryos also exhibit increased expression of the netrin receptors DCC and neogenin that are proposed dependence receptors; however, increased apoptosis was not detected, inconsistent with netrin-1 being an essential dependence receptor ligand in the embryonic spinal cord.

INTRODUCTION

Netrin-1 is a secreted protein that regulates cell migration, cell-cell interactions, and cell-extracellular matrix adhesion during the embryonic development of multiple tissues, including the nervous system, vasculature, lung, pancreas, muscle, and mammary gland (Lai Wing Sun et al., 2011). Roles for netrin-1 have also been addressed in postnatal development and adults (Horn et al., 2013; Jarjour et al., 2008; Shatzmiller et al., 2008); however, these studies have been limited by the death of existing netrin-1 loss-of-function mice shortly after birth (Serafini et al., 1996) and the absence of a conditional *netrin-1* allele. Furthermore, the gene-trap line (*netrin-1*$^{\beta geo}$) that has been used to study netrin-1 loss of function contains a β-galactosidase transgene inserted in the second intron of the *netrin-1* gene (Skarnes et al., 1995). This results in the expression of a truncated netrin-1-β-galactosidase chimeric protein that includes the amino-terminal half of netrin-1. Topologically, the protein chimera presents the netrin-1 sequence on the extracellular face of the plasma membrane, raising the possibility that residual netrin-1 function may persist, even in mice homozygous for the insertion. In addition, alternative mRNA splicing around the inserted sequence results in the generation of a small amount of wild-type full-length netrin-1 mRNA, even in homozygous mutants (Serafini et al., 1996). Thus, the *netrin-1*$^{\beta geo}$ mice are hypomorphs that likely maintain some level of residual netrin-1 function.

Netrin-1 has also been proposed to function as an anti-apoptotic factor, with its receptors deleted in colorectal cancer (DCC) and the Unc5 homologs functioning as "dependence receptors" that trigger cell death in the absence of ligand (Llambi et al., 2001; Mehlen and Guenebeaud, 2010; Mehlen et al., 1998). While evidence for netrin-1 supporting cell survival has been provided, the "dependence receptor" mechanism of action remains controversial. For example, Llambi et al. (2001) and Furne et al. (2008) reported increased apoptosis in the brainstem and spinal cord of *netrin-1*$^{\beta geo/\beta geo}$ embryos, while Williams et al. (2006) detected no change. Furthermore, in vivo studies of apoptosis using the *netrin-1*$^{\beta geo}$ mouse line are confounded by possible toxic gain-of-function effects caused by the expression of the mutant netrin-1-β-galactosidase protein chimera that aggregates inside cells (Shatzmiller et al., 2008). This potential gain-of-function toxicity, together with the residual levels of wild-type netrin-1 protein expressed in *netrin-1*$^{\beta geo/\beta geo}$ homozygotes, supports the critical need to generate an unambiguous *netrin-1* null allele.

Here, we report the generation and initial characterization of a conditional *netrin-1* allele (*netrin-1*^{flox}) produced by introducing flanking *loxP* sequences around the first coding exon of the

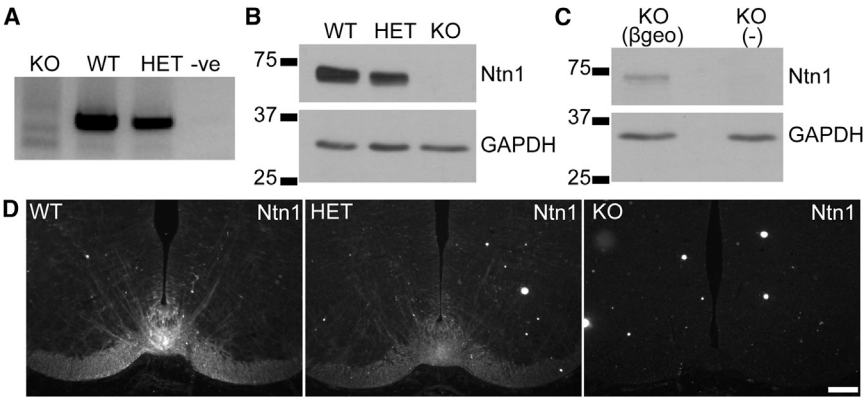

Figure 1. Generation and Validation of *netrin-1*$^{-/-}$ Knockout Mice

(A) RT-PCR confirming loss of netrin-1 mRNA in *netrin-1*$^{-/-}$ knockout animals.

(B) Western blot of protein homogenate collected from E14.5 spinal cord. No netrin-1 protein is detected in the *netrin-1*$^{-/-}$ knockouts, and reduced levels of netrin-1 are detected in heterozygotes.

(C) Western blot of protein homogenate collected from E14.5 spinal cord comparing netrin-1 protein levels in *netrin-1*$^{\beta geo/\beta geo}$ knockouts and *netrin-1*$^{-/-}$ knockouts. The *netrin-1*$^{\beta geo/\beta geo}$ knockout expresses low levels of wild-type netrin-1 protein.

(D) Netrin-1 staining of E12.5 spinal cord where netrin-1 is expressed at the floor plate. No netrin-1 protein is detected in *netrin-1*$^{-/-}$ knockout mice, and reduced levels are detected in heterozygous mice. Scale bar, 50 μm.

netrin-1 gene. By germline expression of cre, we then generated a *netrin-1* null allele (*netrin-1*$^{-}$). Complete loss of netrin-1 function results in embryonic death by approximately embryonic day 14.5 (E14.5), revealing a substantially more severe phenotype than that of *netrin-1*$^{\beta geo/\beta geo}$ homozygotes, which die within a few hours after birth. Analysis of the embryonic spinal cord revealed that *netrin-1*$^{-/-}$ knockouts exhibit severe neural-developmental defects that include almost complete absence of the ventral commissure, disrupted dorsal root entry zone, and an enlarged central canal. Levels of DCC and neogenin protein are increased in *netrin-1*$^{-/-}$ knockout mice; however, in spite of the increased receptor expression and absence of netrin-1 protein, no increased cell death was detected, providing strong evidence that netrin-1 is not an essential dependence ligand for cell survival in the embryonic spinal cord.

RESULTS

Generation of the Netrin-1 Null Mouse Line

To assess the consequences of complete loss of netrin-1 function, we generated a conditional *netrin-1* allele by introducing two unidirectional *loxP* sites flanking the first coding exon of the *netrin-1* gene (*netrin-1*^{flox}). Germline deletion of *netrin-1* was then achieved by crossing *netrin-1*$^{flox/+}$ mice to a *CMVcre* line, which expresses cre ubiquitously in all cells (Schwenk et al., 1995). This resulted in the generation of *netrin-1*$^{+/-}$ heterozygotes, which were crossed to generate *netrin-1*$^{-/-}$ knockout animals. The absence of the floxed *netrin-1* mRNA in *netrin-1*$^{-/-}$ embryos was confirmed using RT-PCR (Figure 1A). The resulting loss of netrin-1 protein was verified by the absence of netrin-1 on western blots of E14.5 spinal cord homogenates (a tissue with abundant netrin-1 expression), as well as by the complete absence of netrin-1 protein detected immunohistochemically at the embryonic spinal floor plate (Figures 1B and 1D). Unlike *netrin-1* $^{\beta geo/\beta geo}$ homozygous mice, which western blot analyses reveal express ~1%–5% of the level of full-length netrin-1 protein found in wild-type embryonic brain and spinal cord homogenates, absolutely no netrin-1 protein was detected in *netrin-1*$^{-/-}$ embryos (Figure 1C). A gene-dosage effect was observed, with *netrin-1*$^{+/-}$ heterozygous animals expressing less netrin-1 protein than wild-type littermates (Figure 1B,D).

Netrin-1$^{-/-}$ Knockout Mice Exhibit a More Severe Phenotype Than Netrin-1 $^{\beta geo/\beta geo}$ Mice

Homozygous *netrin-1*$^{\beta geo/\beta geo}$ mice die shortly after birth (Serafini et al., 1996). We therefore examined litters of newborn pups from *netrin-1*$^{+/-}$ crosses, but in no instance were newborn *netrin-1*$^{-/-}$ pups obtained. Assessment of the genetic makeup of litters at earlier stages of development revealed that complete loss of netrin-1 results in embryonic lethality by ~E14.5. Thus, the netrin-1 null phenotype is substantially more severe than that of the *netrin-1*$^{\beta geo/\beta geo}$ mutant (Serafini et al., 1996).

Netrin-1$^{\beta geo/\beta geo}$ homozygous embryos exhibit severe neural-developmental CNS deficits (Serafini et al., 1996). Similar to these mice, examination of the developing spinal cord of *netrin-1*$^{-/-}$ embryos at E10.5, E12.5, and E14.5 revealed the nearly complete absence of the ventral spinal commissure (Figures 2A–2D), a defect resulting from the misguidance of spinal commissural axons (Serafini et al., 1996). The average dorsal-ventral height of the commissure in E14.5 *netrin-1*$^{-/-}$ embryos was 7.6 ± 0.81 μm, compared to 66.5 ± 3.19 μm in wild-types (Figure 2G). Assuming an average axonal diameter of 1 μm, this indicates that only very few axons successfully cross the midline to form a residual ventral commissure in *netrin-1*$^{-/-}$ embryos. Interestingly, compared to *netrin-1*$^{\beta geo/\beta geo}$ homozygous embryos (Watanabe et al., 2006), *netrin-1*$^{-/-}$ embryos exhibit a substantially more disrupted dorsal root entry zone (Figure 2H), which can be attributed to the misguidance of sensory axons projecting from the dorsal root ganglia (DRG) into the dorsal spinal cord (Masuda et al., 2008; Watanabe et al., 2006). TrkA-positive sensory axons were also observed to inappropriately invade the spinal cord, projecting horizontally toward the central canal (Figure 2I). In addition, we noted mislocalized longitudinal axon bundles (Figure 2C) and thinning of the ventricular zone in E14.5 *netrin-1*$^{-/-}$ embryos (Figures 2C and 2D). While the cross-sectional surface area of the *netrin-1*$^{-/-}$ spinal cord, excluding the central canal, did not differ compared to control littermates, the central canal was significantly larger in *netrin-1*$^{-/-}$ embryos at E14.5 (Figures 2C–2F).

Loss of Netrin-1 Does Not Alter Cell-type Specification in Early Spinal Cord

To determine whether netrin-1 contributes to cell fate specification and early patterning in the spinal cord, a detailed

immunohistochemical analysis of progenitor and postmitotic markers was carried out on E11.5 brachial spinal cord sections. The specification of spinal progenitors was assessed by comparing the expression of Nkx2.2 (Figure 3A), Olig2 (Figure 3B), and Pax7 (Figure 3C), which label progenitors destined to become V3 interneurons, motor neurons, and dorsal sensory interneurons, respectively (Ericson et al., 1997; Novitch et al., 2001). The Pax7 expression domain is seemingly unaltered in its composition and positioning. While the number of cells expressing Olig2 and Nkx2.2 remains unaltered in the absence of netrin-1, the Olig2 progenitor population is more ventrally positioned and the Nkx2.2 population is more laterally displaced. These differences in progenitor localization appear to result from the absence of descending commissural axons.

The Lim homeobox transcription factors Isl1/2 and Lim1 are broadly expressed in postmitotic spinal neurons at E11.5 and therefore allow for a general assessment of postmitotic differentiation. Additionally, these proteins are differentially expressed in the two subdivisions of the lateral motor column (LMC), with Isl1/2 expressed in medial LMC and Lim1 expressed in lateral LMC motor neurons (Tsuchida et al., 1994). The broad expression and positioning of these markers remained unaltered in the absence of netrin-1 (Figure 3B). The number of Isl1/2-expressing medial LMC neurons was unchanged, but their distribution within the LMC appeared shifted (Figure 3B). The transcription factor Lmx1b labels the dI5 post-mitotic interneurons in the E11.5 spinal cord (Müller et al., 2002). Cell counts revealed that the number of Lmx1b-expressing cells remains unchanged in the absence of netrin-1, but the distribution of these cells appears altered, possibly due to the absence of descending commissural axons (Figure 3D). We conclude that the absence of the spinal ventral commissure may slightly alter the positions of some cells, but we detected no evidence that the absence of netrin-1 alters cell fate specification or early patterning of the embryonic spinal cord.

Loss of Netrin-1 Results in Increased DCC and Neogenin Expression but Does Not Increase Cell Death

Immunostaining embryonic spinal cords for the netrin-1 receptors DCC and neogenin revealed a substantial increase in both proteins in the absence of netrin-1 (Figures 4A and 4C). This was confirmed by western blot analysis of spinal cord homogenates from E14.5 *netrin-1*$^{-/-}$ knockout and wild-type littermates (Figures 4B and 4D). DCC and Unc5 homologs have been reported to regulate cell survival and to function as dependence receptors (Llambi et al., 2001; Mehlen and Guenebeaud, 2010; Mehlen et al., 1998); however, the literature is controversial regarding whether loss of netrin-1 protein promotes cell death (Furne et al., 2008; Llambi et al., 2001; Williams et al., 2006). In particular, it is not clear whether reports of cell death in *netrin-1*$^{\beta geo/\beta geo}$ homozygous mice are the consequence of loss of netrin-1 protein or potentially due to toxicity from the netrin-1-β-galactosidase fusion protein. If DCC indeed functions as a dependence receptor, the absence of netrin-1, as well as the increased DCC expression in netrin-1 null embryos, is predicted to promote the activation of pro-apoptotic signaling. We therefore examined *netrin-1*$^{-/-}$ knockout spinal cords to determine whether complete loss of netrin-1 protein results in increased cell death.

Western blots revealed that E12.5 and E14.5 spinal cord homogenates of *netrin-1*$^{-/-}$ mutants did not contain increased cleaved caspase-3 protein levels (Figures 4E–4G), nor did we detect an increase in the number of cleaved caspase-3-positive cells immunohistochemically in the spinal cord or DRGs at either age (Figures 4H, 4I, and 4L–4O). In line with this, we did not detect an increase in the number of TUNEL-positive cells in either the spinal cord or DRGs of E12.5 or E14.5 *netrin-1*$^{-/-}$ embryos (Figures 4J, 4K, and 4P–4S). We conclude that loss of netrin-1 does not result in increased cell death in the embryonic spinal cord or DRGs of *netrin-1*$^{-/-}$ knockout mice.

DISCUSSION

We report the generation of a complete netrin-1 null animal by deleting the first coding exon of *netrin-1*, which abolishes the expression of netrin-1 protein. Complete loss of netrin-1 resulted in a substantially more severe phenotype than documented in the previously reported *netrin-1*$^{\beta geo}$ gene-trap mouse line (Serafini et al., 1996), with *netrin-1*$^{-/-}$ knockout mice dying at ~E14.5 in contrast to the *netrin-1*$^{\beta geo/\beta geo}$ hypomorphs that die shortly after birth. The cause of the embryonic death is currently unknown, but it coincides with the embryonic lethality of mice null for the netrin-1 receptor Unc5B (Lu et al., 2004), which likely die from defects in vascular development. Notably, death at this age corresponds to a developmental period during which defects of the heart or placenta often lead to embryonic lethality (Savolainen et al., 2009). Axon guidance defects in the developing spinal cord were consistent with, but more severe than, those documented in homozygous *netrin-1*$^{\beta geo}$ gene trap mice. A prominent difference is the increased severity of sensory axons mistargeted in the dorsal spinal cord, which are normally restrained by netrin-1 (Watanabe et al., 2006). Together, our results support the conclusion that the *netrin-1*$^{\beta geo}$ mouse line retains residual netrin-1 function. Thus, the *netrin-1* null line reported here will be a critical tool for future studies examining the consequences of complete loss of netrin-1 function. Furthermore, the *netrin-1*^{flox} mice will be important for the analysis of netrin-1 function in specific cell types and the capacity to extend the analysis of netrin-1 loss of function into adult animals.

Our data also demonstrate that netrin-1 is essential for the vast majority of commissural axons to reach the ventral midline. Both Sonic hedgehog (Shh) and vascular endothelial growth factor (VEGF) have been identified as additional chemoattractants for commissural axon guidance (Charron et al., 2003; Ruiz de Almodovar et al., 2011). However, while disruption of Shh or VEGF function causes ventrally projecting commissural axons to wander laterally, these defects are relatively minor and most, if not all, commissural axons ultimately reach the floor plate and cross the midline. In contrast, in the absence of netrin-1, the vast majority of commissural axons do not reach the ventral midline. We speculate that at least two non-exclusive mechanisms may contribute to the capacity of the few remaining axons to cross. These axons may project from cell bodies located relatively close to the ventral midline that therefore have a higher probability of encountering the floor

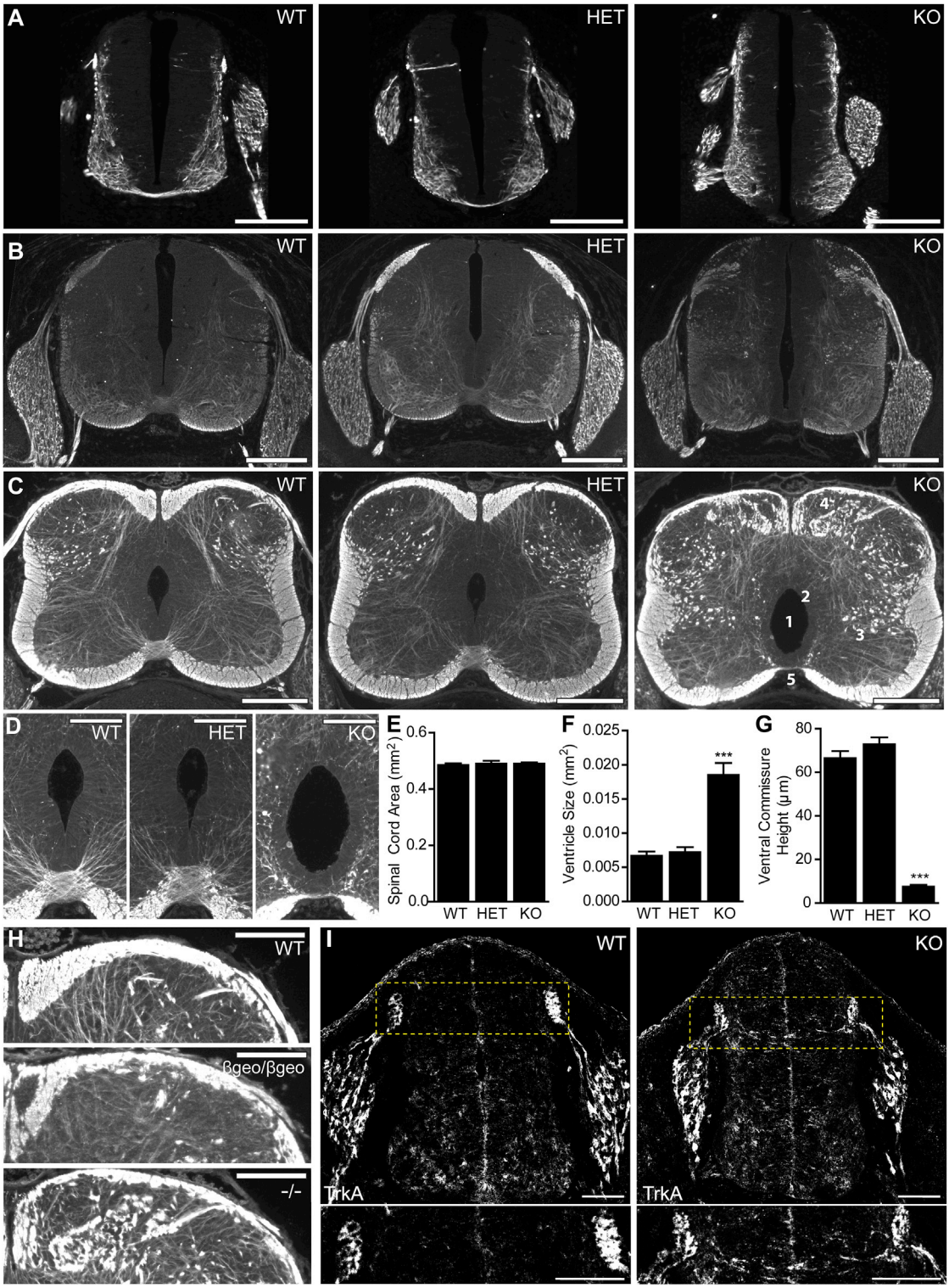

Figure 2. *Netrin-1*$^{-/-}$ Knockout Spinal Cords

(A–C) Representative spinal cord sections at E10.5 (NFM) (A), 12.5 (NFM) (B), and E14.5 (SMI-312) (C). Multiple defects are apparent in *netrin-1*$^{-/-}$ knockout spinal cords, including (1) a larger central canal, (2) thinning of the ventricular zone surrounding the central canal, (3) mislocalized axon bundles, (4) a disorganized dorsal root entry zone, and (5) nearly complete loss of ventral commissure.

(D) Magnification of ventral commissure and central canal in (C).

(legend continued on next page)

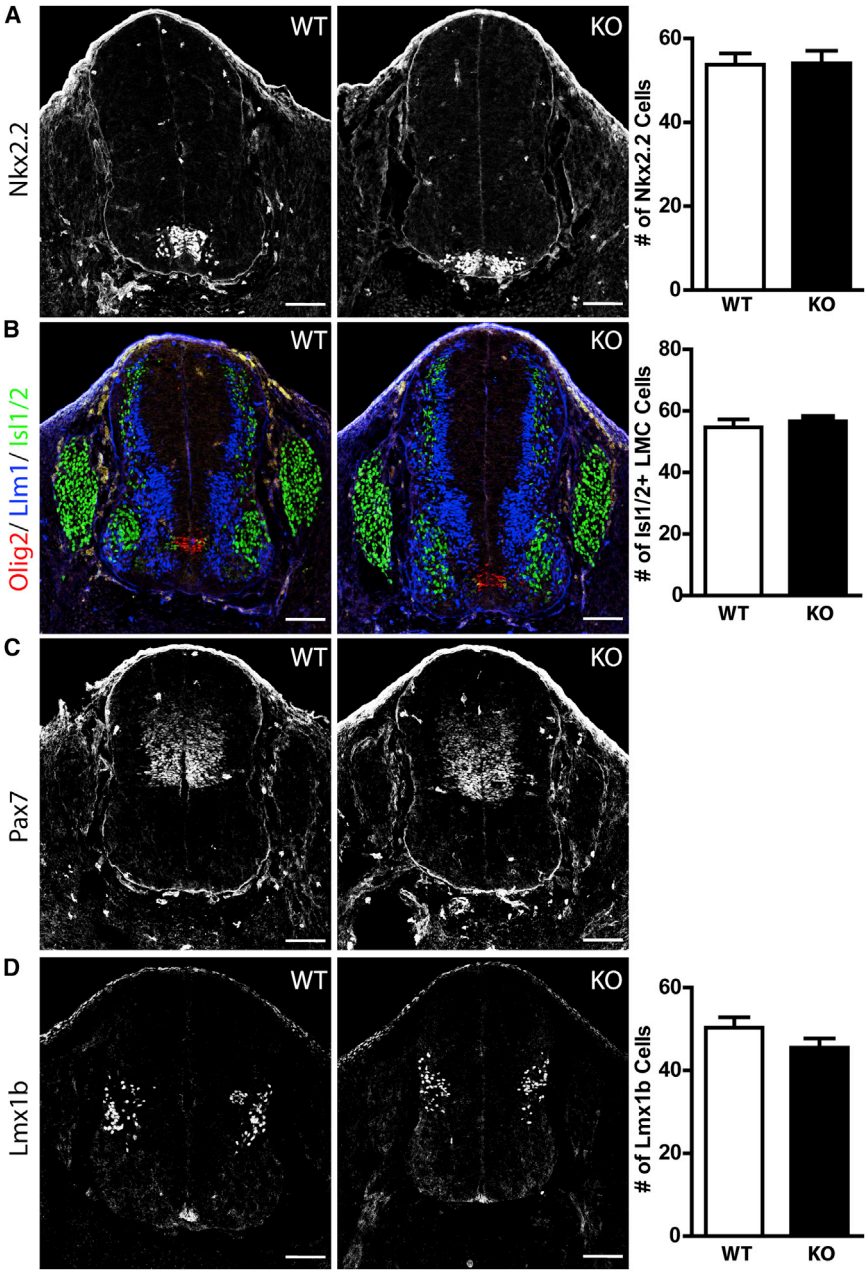

Figure 3. Cell-Fate Specification and Early Patterning in E11.5 Brachial Spinal Cord

(A) Expression of Nkx2.2 reveals that the number of positive cells is unaltered in *netrin-1*$^{-/-}$ knockouts.

(B) Expression of Olig2, Lim1, and Isl1/2 spinal progenitors. *Netrin-1*$^{-/-}$ knockout embryos display a more ventrally positioned distribution of Olig2 positive cells. Quantification of Isl1/2+ cells in the lateral motor column (LMC) reveals no difference in the knockout.

(C) Expression of Pax7 in spinal progenitors is undisturbed in *netrin-1*$^{-/-}$ knockout mice.

(D) Expression and quantification of Lmx1b+ cells remains unaltered in *netrin-1*$^{-/-}$ knockout mice.

Data are presented as mean ± SEM.

plate by chance. Alternatively, these axons may correspond to a subpopulation of commissural neurons that utilize a netrin-1 independent mechanism to target the ventral midline.

Our findings also revealed that the absence of netrin-1 results in a substantial increase in DCC and neogenin protein. It has been reported that application of netrin-1 to neurons in culture results in DCC ubiquitination and proteosomal degradation (Kim et al., 2005), but a correlate in vivo has not previously been described. The increased levels of DCC protein in our *netrin-1*$^{-/-}$ knockouts may be due to decreased ligand-dependent degradation. Importantly, this indicates that netrin-1 null mice may exhibit phenotypes that are not directly due to netrin-1 loss of function but rather the result of DCC or neogenin gain of function. In addition to signaling induced by binding netrin-1, DCC binds other ligands, including netrin-3, netrin-4, draxin (Ahmed et al., 2011), and cerebellin 4 (CBLN4) (Haddick et al., 2014; Wei et al., 2012), while neogenin binds members of the repulsive guidance molecule (RGM) family (Rajagopalan et al., 2004).

Furthermore, based on the pro-apoptotic dependence receptor hypothesis, which postulates that in the absence of ligand a dependence receptor will activate apoptosis, the increased level of DCC protein in *netrin-1*$^{-/-}$ embryos is predicted to exacerbate cell death. In contrast to this prediction and to previous reports using *netrin-1*$^{\beta geo/\beta geo}$ homozygous gene-trap mice (Furne et al., 2008; Llambi et al., 2001), we did not detect increased apoptosis in the embryonic spinal cord or DRGs of *netrin-1*$^{-/-}$ embryos, in spite of substantially increased DCC and neogenin expression. Although we have not ruled out the

(E) No difference in the cross-sectional area of knockout spinal cords (spinal cord area − central canal area; n = 4–6).

(F) Larger central canal in *netrin-1*$^{-/-}$ knockout animals (n = 4–6, ***p < 0.0001).

(G) Quantification of the dorsal-ventral height of the ventral commissure (n = 4–6, ***p < 0.0001).

(H) Comparison of dorsal root entry zone in wild-type, *netrin-1*$^{\beta geo/\beta geo}$, and *netrin-1*$^{-/-}$ knockout embryos at E14.5.

(I) TrkA immunoreactivity reveals inappropriate invasion of TrkA-expressing sensory axons within the spinal cord in *netrin-1*$^{-/-}$ knockouts (n = 3–4).

Scale bars represent 200 μm (A–C) and 100 μm (D, H, and I). Data are presented as mean ± SEM.

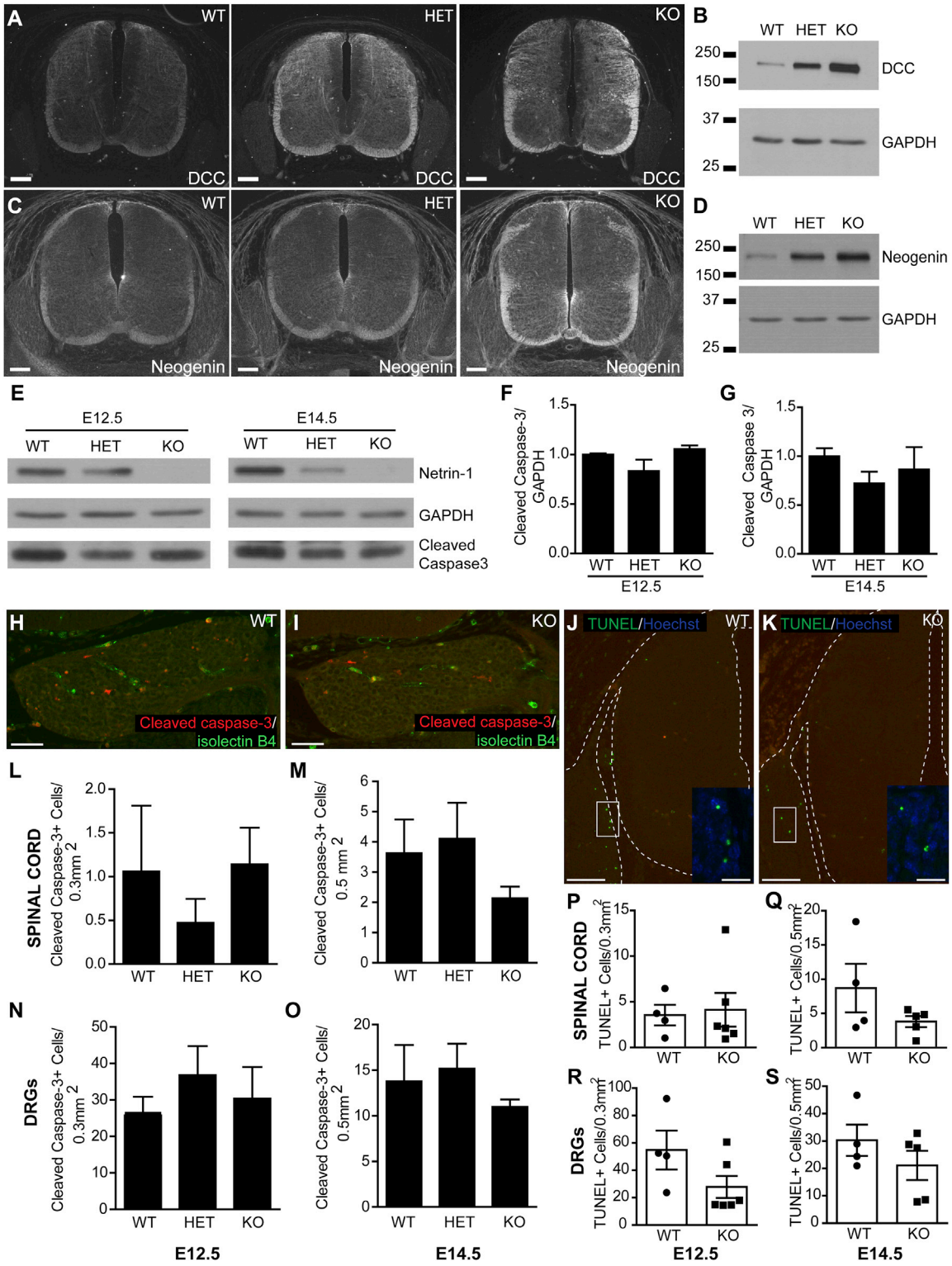

Figure 4. Loss of Netrin-1 Results in Increased DCC and Neogenin Protein Expression but Does Not Increase Cell Death

(A) Immunohistochemistry of E12.5 spinal cord shows DCC protein expression increases in a reciprocal fashion with the decrease in number of *netrin-1* alleles.

(B) Western blot of protein homogenate from E14.5 spinal cord shows the same increase in DCC protein levels.

(C) Immunohistochemistry of E12.5 spinal cord shows neogenin protein expression increases in *netrin-1*$^{-/-}$ knockout embryos.

(D) Western blot of protein homogenate from E14.5 spinal cord showing increased neogenin protein levels in *netrin-1*$^{-/-}$ knockout embryos.

(legend continued on next page)

possibility that netrin-1 may influence apoptosis in other CNS regions, these findings argue strongly against the conclusion that netrin-1 functions as an essential dependence ligand in the embryonic spinal cord.

EXPERIMENTAL PROCEDURES

Generation of the *Netrin-1^{flox}* Allele

Genomic DNA corresponding to the *netrin-1* locus was isolated from a C57BL/6J mouse genomic BAC (NCBI CloneDB: RP23-231D12). The necessary genomic elements were amplified by PCR and cloned into the targeting vector pCOM-True (Reich et al., 2011). A 1,529-bp genomic region, containing the entire first coding exon of *netrin-1*, along with 66 bp of 5′ UTR, was amplified by PCR. The amplified product was inserted between two *loxP* sequences of pCOM-True at the *Mfe*I/*Asc*I site. A 1,204-bp 5′ homology arm was amplified by PCR and inserted in front of the first *loxP* sequence at the *Xho*I/*Spe*I site. A 5,232-bp 3′ homology arm was amplified by PCR and inserted after the second *loxP* site and *frt* site flanking the neomycin resistance gene (*NeoR*). All genomic elements of the targeting construct were verified by sequencing. The targeting construct was linearized with *Xho*I and electroporated into 129R1 ES cells. ES cell clones resistant to G418 were expanded and analyzed for homologous recombination using nested PCR. Correctly targeted clones were identified and karyotyped. One clone was selected based on karyotyping results and injected into C57BL/6-derived blastocysts. The resulting chimeras from this clone produced germline offspring. See Supplemental Experimental Procedures for primer sequences.

Generation of *Netrin-1^{flox}* and *Netrin-1$^{-/-}$* Mice

Positively selected *netrin-1$^{flox/+}$* chimeric mice were crossed to a FLPe recombinase-expressing mouse line, B6;SJL-Tg(ACTFLPe)9205Dym/J, to remove *Neo^{R}* between the two *frt* sites and produce the *netrin-1^{flox}* allele. To generate the *netrin-1$^{+/-}$* mice, we crossed the *netrin-1$^{flox/+}$* mice to a CMVcre-expressing mouse line, B6.C-Tg (CMV-cre)1Cgn/J (Schwenk et al., 1995). Primers used for genotyping are available in Supplemental Experimental Procedures.

RT-PCR

RNA was purified from E11.5 mouse embryos using RNeasy Mini Kit (QIAGEN). cDNA was produced using SuperScript III First-Strand Synthesis System for RT-PCR (Invitrogen) using Oligo(dT)$_{20}$ primers. The following primers were used to amplify netrin-1 mRNA: 5′-GCTGCAAGTGCAACGGCCAC-3′ and 5′-ATCGGTTGCAGGTGATGCCC-3′.

Immunohistochemistry

Embryos were fixed in Carnoy's fixative (60% ethanol, 10% acetic acid, and 30% chloroform) for 2 hr at room temperature, followed by two 20-min washes in 100% ethanol. Tissue was then incubated for 1 hr in toluene before transferring to paraffin overnight at 60°C. The following day, embryos were embedded in clean paraffin and 10 μm sections cut on a microtome. Prior to staining, tissue sections were rehydrated. They were blocked 1 hr in 3% BSA, 3% heat-inactivated horse serum (HIHS), 0.3% Triton X-100 in PBS. Primary antibodies diluted in blocking solution were incubated with tissue sections overnight at 4°C. Tissue was washed three times (10 min each) in PBS, incubated for 1 hr at room temperature with secondary antibodies diluted in 3% BSA and 3% HIHS in PBS, then washed three times (10 min each) in PBS. Slides were then rinsed with water and mounted with Fluoromount G (Southern Biotech). Staining was imaged using a Zeiss Axiovert S100TV microscope and Magnifire CCD camera (Optronics). For netrin-1 and cleaved caspase-3 antibodies, antigen retrieval was performed prior to blocking by boiling the tissue sections in citrate buffer (pH 6.0) for 20 min. HIHS was omitted when staining with netrin-1 antibody.

To assess cell fate and patterning in the embryonic spinal cord, E11.5 embryos were fixed in 4% paraformaldehyde (PFA) for 1.5 hr, rinsed thoroughly in PBS, and cryoprotected overnight in 30% sucrose PBS at 4°C. Embryos were mounted in optimum cutting temperature (OCT) compound, and 12-μm sections cut with a Leica cryostat. Sections were rehydrated with 0.1% Triton X-100 and 1% HIHS in PBS for 10 min, then primary antibodies diluted in the same solution were added and sections incubated overnight at 4°C. Sections were rinsed thoroughly with PBS and then labeled with secondary antibodies. Sections were mounted in Mowiol mounting medium and imaged using a 10× objective on a Zeiss LSM710 confocal microscope. See Supplemental Experimental Procedures for details of antibodies used.

TUNEL Assay

TUNEL staining was performed on Carnoy's fixed tissue sections (see above) using a DeadEnd Fluorometric TUNEL Kit (Promega) according to the manufacturer's instructions. Staining was imaged using a Zeiss Axiovert S100TV microscope and Magnifire CCD camera (Optronics) and TUNEL-positive cells in the spinal cord and DRGs counted. Because some autofluorescent blood cells were detected, autofluorescent background was subtracted before counting.

Western Blotting

Spinal cords were dissected from E12.5 and E14.5 embryos and homogenized in ice-cold RIPA buffer (10 mM phosphate buffer [pH 7.2], 150 mM NaCl, 1% NP-40, 0.5% sodium deoxycholate, and 0.1% SDS) with protease and phosphatase inhibitors (aprotinin 2 μg/ml, leupeptin 5 μg/ml, EDTA 2 mM, sodium orthovanadate 1 mM, sodium fluoride 1 mM, and PMSF 1 mM). 30 μg of protein was run on SDS-PAGE gels (8% or 12%), transferred onto nitrocellulose, and probed with antibodies. Blots were developed using Immobilon Western Chemiluminescent HRP Substrate (Millipore). Densitometric analysis was performed using Adobe Photoshop. Values were normalized to loading control values for GAPDH.

Statistical Analysis

Statistically analyses were performed using GraphPad Prism software. The Student's t test (two-tailed) or one-way ANOVA with Tukey's post hoc test was used.

SUPPLEMENTAL INFORMATION

Supplemental Information includes Supplemental Experimental Procedures and can be found with this article online at http://dx.doi.org/10.1016/j.celrep.2015.07.028.

AUTHOR CONTRIBUTIONS

J.M.B. designed and performed experiments and wrote the manuscript; D.H. designed and generated mouse lines, designed and performed experiments, and wrote the manuscript; K.L.W.S. performed experiments and edited the manuscript; L.P.C. designed and performed experiments and wrote the

(E) Representative western blots for cleaved caspase-3 in spinal cord homogenates from E12.5 and E14.5 embryo littermates.
(F and G) Quantification of blots did not detect a difference in cleaved caspase-3 protein levels at either age (n = 3 embryos/genotype).
(H and I) Representative cleaved caspase-3 immunohistochemistry in the DRGs of netrin-1 wild-type (H) and knockout (I) embryos.
(J and K) Representative TUNEL staining in the spinal cord and DRGs of netrin-1 wild-type (J) and knockout (K) littermates.
(L–O) No difference in the number of cleaved caspase-3-positive cells was detected in the spinal cord (L and M) or DRGs (N and O) at either E12.5 (L and N) or E14.5 (M and O) (n = 4–6 embryos/genotype).
(P–S) No difference in the number of TUNEL-positive cells was detected in the spinal cord (P and Q) or DRGs (R and S) at either E12.5 (P and R) or E14.5 (Q and S) (n = 4–6 embryos/genotype).
Scale bars represent 100 μm (A, C, J, and K), 50 μm (H and I), and 25 μm (J and K, inset). Data are presented as mean ± SEM.

manuscript; E.D. and J.-F.C. generated mouse lines; A.K. designed experiments and edited the manuscript; and T.E.K. designed experiments and wrote the manuscript.

ACKNOWLEDGMENTS

We thank Ajit Dhaunchak for helpful discussion and assistance. J.M.B. was supported by a Dr. William J. McIlroy Multiple Sclerosis Society of Canada doctoral studentship. D.H. was supported by a Multiple Sclerosis Society of Canada post-doctoral fellowship. K.L.W.S. was supported by a FRQS doctoral scholarship. L.P.C. was supported by a FRQS doctoral scholarship. J.-F.C. was supported by a FRQS Chercheur Sénior award and by grants from CIHR and NSERC. A.K. was supported by grants from the Reseau Québecois de recherche sur la douleur, CIHR, CFI, Brain Canada, and the W. Garfield Weston Foundation. T.E.K. was supported by an FRQS Chercheur Nationaux award and a Killam Foundation Scholar award. The project was supported by grants to T.E.K. from the CIHR and from the Multiple Sclerosis Society of Canada.

Received: March 12, 2015
Revised: May 29, 2015
Accepted: July 14, 2015
Published: August 6, 2015

REFERENCES

Ahmed, G., Shinmyo, Y., Ohta, K., Islam, S.M., Hossain, M., Naser, I.B., Riyadh, M.A., Su, Y., Zhang, S., Tessier-Lavigne, M., and Tanaka, H. (2011). Draxin inhibits axonal outgrowth through the netrin receptor DCC. J. Neurosci. *31*, 14018–14023.

Charron, F., Stein, E., Jeong, J., McMahon, A.P., and Tessier-Lavigne, M. (2003). The morphogen sonic hedgehog is an axonal chemoattractant that collaborates with netrin-1 in midline axon guidance. Cell *113*, 11–23.

Ericson, J., Rashbass, P., Schedl, A., Brenner-Morton, S., Kawakami, A., van Heyningen, V., Jessell, T.M., and Briscoe, J. (1997). Pax6 controls progenitor cell identity and neuronal fate in response to graded Shh signaling. Cell *90*, 169–180.

Furne, C., Rama, N., Corset, V., Chédotal, A., and Mehlen, P. (2008). Netrin-1 is a survival factor during commissural neuron navigation. Proc. Natl. Acad. Sci. USA *105*, 14465–14470.

Haddick, P.C., Tom, I., Luis, E., Quiñones, G., Wranik, B.J., Ramani, S.R., Stephan, J.P., Tessier-Lavigne, M., and Gonzalez, L.C. (2014). Defining the ligand specificity of the deleted in colorectal cancer (DCC) receptor. PLoS ONE *9*, e84823.

Horn, K.E., Glasgow, S.D., Gobert, D., Bull, S.J., Luk, T., Girgis, J., Tremblay, M.E., McEachern, D., Bouchard, J.F., Haber, M., et al. (2013). DCC expression by neurons regulates synaptic plasticity in the adult brain. Cell Rep. *3*, 173–185.

Jarjour, A.A., Bull, S.J., Almasieh, M., Rajasekharan, S., Baker, K.A., Mui, J., Antel, J.P., Di Polo, A., and Kennedy, T.E. (2008). Maintenance of axo-oligodendroglial paranodal junctions requires DCC and netrin-1. J. Neurosci. *28*, 11003–11014.

Kim, T.H., Lee, H.K., Seo, I.A., Bae, H.R., Suh, D.J., Wu, J., Rao, Y., Hwang, K.G., and Park, H.T. (2005). Netrin induces down-regulation of its receptor, Deleted in Colorectal Cancer, through the ubiquitin-proteasome pathway in the embryonic cortical neuron. J. Neurochem. *95*, 1–8.

Lai Wing Sun, K., Correia, J.P., and Kennedy, T.E. (2011). Netrins: versatile extracellular cues with diverse functions. Development *138*, 2153–2169.

Llambi, F., Causeret, F., Bloch-Gallego, E., and Mehlen, P. (2001). Netrin-1 acts as a survival factor via its receptors UNC5H and DCC. EMBO J. *20*, 2715–2722.

Lu, X., Le Noble, F., Yuan, L., Jiang, Q., De Lafarge, B., Sugiyama, D., Bréant, C., Claes, F., De Smet, F., Thomas, J.L., et al. (2004). The netrin receptor UNC5B mediates guidance events controlling morphogenesis of the vascular system. Nature *432*, 179–186.

Masuda, T., Watanabe, K., Sakuma, C., Ikenaka, K., Ono, K., and Yaginuma, H. (2008). Netrin-1 acts as a repulsive guidance cue for sensory axonal projections toward the spinal cord. J. Neurosci. *28*, 10380–10385.

Mehlen, P., and Guenebeaud, C. (2010). Netrin-1 and its dependence receptors as original targets for cancer therapy. Curr. Opin. Oncol. *22*, 46–54.

Mehlen, P., Rabizadeh, S., Snipas, S.J., Assa-Munt, N., Salvesen, G.S., and Bredesen, D.E. (1998). The DCC gene product induces apoptosis by a mechanism requiring receptor proteolysis. Nature *395*, 801–804.

Müller, T., Brohmann, H., Pierani, A., Heppenstall, P.A., Lewin, G.R., Jessell, T.M., and Birchmeier, C. (2002). The homeodomain factor lbx1 distinguishes two major programs of neuronal differentiation in the dorsal spinal cord. Neuron *34*, 551–562.

Novitch, B.G., Chen, A.I., and Jessell, T.M. (2001). Coordinate regulation of motor neuron subtype identity and pan-neuronal properties by the bHLH repressor Olig2. Neuron *31*, 773–789.

Rajagopalan, S., Deitinghoff, L., Davis, D., Conrad, S., Skutella, T., Chedotal, A., Mueller, B.K., and Strittmatter, S.M. (2004). Neogenin mediates the action of repulsive guidance molecule. Nat. Cell Biol. *6*, 756–762.

Reich, A., Spering, C., Gertz, K., Harms, C., Gerhardt, E., Kronenberg, G., Nave, K.A., Schwab, M., Tauber, S.C., Drinkut, A., et al. (2011). Fas/CD95 regulatory protein Faim2 is neuroprotective after transient brain ischemia. J. Neurosci. *31*, 225–233.

Ruiz de Almodovar, C., Fabre, P.J., Knevels, E., Coulon, C., Segura, I., Haddick, P.C., Aerts, L., Delattin, N., Strasser, G., Oh, W.J., et al. (2011). VEGF mediates commissural axon chemoattraction through its receptor Flk1. Neuron *70*, 966–978.

Savolainen, S.M., Foley, J.F., and Elmore, S.A. (2009). Histology atlas of the developing mouse heart with emphasis on E11.5 to E18.5. Toxicol. Pathol. *37*, 395–414.

Schwenk, F., Baron, U., and Rajewsky, K. (1995). A cre-transgenic mouse strain for the ubiquitous deletion of loxP-flanked gene segments including deletion in germ cells. Nucleic Acids Res. *23*, 5080–5081.

Serafini, T., Colamarino, S.A., Leonardo, E.D., Wang, H., Beddington, R., Skarnes, W.C., and Tessier-Lavigne, M. (1996). Netrin-1 is required for commissural axon guidance in the developing vertebrate nervous system. Cell *87*, 1001–1014.

Shatzmiller, R.A., Goldman, J.S., Simard-Emond, L., Rymar, V., Manitt, C., Sadikot, A.F., and Kennedy, T.E. (2008). Graded expression of netrin-1 by specific neuronal subtypes in the adult mammalian striatum. Neuroscience *157*, 621–636.

Skarnes, W.C., Moss, J.E., Hurtley, S.M., and Beddington, R.S. (1995). Capturing genes encoding membrane and secreted proteins important for mouse development. Proc. Natl. Acad. Sci. USA *92*, 6592–6596.

Tsuchida, T., Ensini, M., Morton, S.B., Baldassare, M., Edlund, T., Jessell, T.M., and Pfaff, S.L. (1994). Topographic organization of embryonic motor neurons defined by expression of LIM homeobox genes. Cell *79*, 957–970.

Watanabe, K., Tamamaki, N., Furuta, T., Ackerman, S.L., Ikenaka, K., and Ono, K. (2006). Dorsally derived netrin 1 provides an inhibitory cue and elaborates the 'waiting period' for primary sensory axons in the developing spinal cord. Development *133*, 1379–1387.

Wei, P., Pattarini, R., Rong, Y., Guo, H., Bansal, P.K., Kusnoor, S.V., Deutch, A.Y., Parris, J., and Morgan, J.I. (2012). The Cbln family of proteins interact with multiple signaling pathways. J. Neurochem. *121*, 717–729.

Williams, M.E., Lu, X., McKenna, W.L., Washington, R., Boyette, A., Strickland, P., Dillon, A., Kaprielian, Z., Tessier-Lavigne, M., and Hinck, L. (2006). UNC5A promotes neuronal apoptosis during spinal cord development independent of netrin-1. Nat. Neurosci. *9*, 996–998.